JOURNAL OF AIRCRAFT
Vol. 48, No. 5, September–October 2011

Engineering Notes

Stall Warning Using Flap Hinge Moment Measurements

Phillip J. Ansell* and Michael B. Bragg†
University of Illinois at Urbana–Champaign, Urbana, Illinois 61801
and
Michael F. Kerho‡
Rolling Hills Research Corporation, El Segundo, California 90245

DOI: 10.2514/1.C031435

Introduction

GENERALLY, surface contamination of a wing leads to reductions in performance [1–3]. Premature stall due to contamination can also have devastating effects on the controllability of aircraft [4,5]. Currently, there is no established, effective method for monitoring aircraft performance and controllability in order to prevent stall under adverse conditions created by surface contamination. While angle-of-attack sensors are capable of providing an effective stall warning for an aircraft free of contaminants, the effectiveness of such systems greatly diminishes with the presence of contaminants on an aircraft wing.

Gurbacki and Bragg [6] studied the steady and unsteady hinge moment behaviors of supercooled large-droplet ice-induced stall on a NACA 23012 airfoil model with a simple flap. In that study, it was found that the rms of the unsteady hinge moment increased 1 to 3° angles of attack before stall for the iced case. Thus, it was identified that the unsteady separated flow led to unsteady changes in the hinge moment, giving rise to the concept that unsteady hinge moment measurements could be used to predict ice-induced stall [7].

Such a method could be further applied to a system capable of monitoring aircraft aerodynamic performance and providing real-time predictions of the edge of a flight envelope. In addition to flight beyond the baseline-clean aircraft flight envelope, such a system could potentially detect a reduction in the envelope due to several in-flight environmental contaminants resulting from icing encounters, heavy rain, surface contamination in the form of roughness, and structural damage, such as bird strikes or battle damage. To further this concept, additional development is needed beyond the initial work of Gurbacki and Bragg [6].

This Note reports the further development of such a technique. The specific focus of this Note is the development of a detection algorithm using the unsteady hinge moment from a simple flap on an airfoil with and without contaminants. The algorithm developed is used to predict stall several degrees before the event.

Detection Algorithm Development

To obtain hinge moment data to be used in the detection algorithm development, a series of wind-tunnel tests were performed at the University of Illinois at Urbana–Champaign on a flapped NACA 3415 model [8]. In addition to the clean airfoil configuration, a series of six contaminated airfoil configurations were tested. These contamination configurations included both leading-edge glaze-ice and rime-ice simulations, two levels of leading-edge roughness, and both simulated three-dimensional (3-D) leading-edge damage and 3-D upper-surface damage cases. All cases were tested at Reynolds numbers of 1.8×10^6 ($M = 0.18$) and 1.0×10^6 ($M = 0.1$) at flap deflections of 0°, ±5°, and ±10°. Hinge moment measurements were acquired at a sample rate of 3 kHz for 10 s. Before applying the hinge moment data to the stall detection algorithm, the hinge moment measurements were digitally low-pass filtered at 50 Hz to minimize the influence of structural frequencies.

The unsteady hinge moment data obtained from the NACA 3415 test were operated on to increase the signal-to-noise ratio to provide more reliable estimates of the stall angle of attack. The system used a combination of three separate detector function algorithms to provide stall warning information. The first method calculated the moment about the mean of the unsteady hinge moment signal to the fourth order, denoted as the moment-based detector function. The second method used a time-derivative-based function of the unsteady hinge moment signal, denoted as the derivative-based detector function. The third method integrated the power spectral density function of the hinge moment signal from 0.1 to 50 Hz, denoted as the spectrum-based detector function.

A sample output of the three detector functions for $Re = 1.8 \times 10^6$ and $\delta_f = 0°$ is shown in Fig. 1, with a vertical line indicating α_{stall}. From Fig. 1, each of the detector functions produced a relatively smooth output, which significantly increased in magnitude several degrees before stall. Above $\alpha = 0°$, the functions provide an almost monotonic increase in level with increasing angle of attack up to stall. In addition to increasing magnitudes as stall is approached, the slope of each of the detector functions is also shown to increase. Using a threshold-based approach, the three detector functions appear to provide sufficient output and a large enough signal-to-noise ratio to be used as accurate predictive indicators of stall.

For the detection algorithms to be useful in predicting stall, the algorithms must provide a consistent output across the widest range of environmental conditions, including icing, surface roughness contamination, bird strikes, heavy rain, etc. If the output is not consistent across these different hazards, a simple threshold-based approach would prove inadequate, producing inconsistent results dependent upon the hazard. A plot showing the output of the moment-based detector function for the clean NACA 3415 model and the model with all six tested simulated contaminants as a function of angle of attack before stall ($\alpha - \alpha_{\text{stall}}$) at $Re = 1.8 \times 10^6$ and $\delta_f = 0°$ is shown in Fig. 2. The outputs of the other two detector functions are similar in nature and can be seen in Ansell et al. [9] From Fig. 2, the output for the moment-based detector function for the clean model and the model with five of the simulated contaminants collapse onto a single curve. The one exception is the simulated upper-surface damage case, which was the only non-leading-edge contamination case studied.

The difference in detector function output of the simulated upper-surface damage case was attributed to the size and 3-D nature of the contamination and its midchord placement on the model. The 3-D simulated upper-surface damage mimics the effect of an isolated

Presented as Paper 2010-4225 at the 28th AIAA Applied Aerodynamics Conference, Chicago, IL, 28 July–1 June 2010; received 4 March 2011; revision received 11 May 2011; accepted for publication 24 May 2011.

*Graduate Research Assistant, Department of Aerospace Engineering. Member AIAA.
†Professor of Aerospace Engineering, Executive Associate Dean for Academic Affairs. Fellow AIAA.
‡Chief Aerodynamicist. Associate Fellow AIAA.

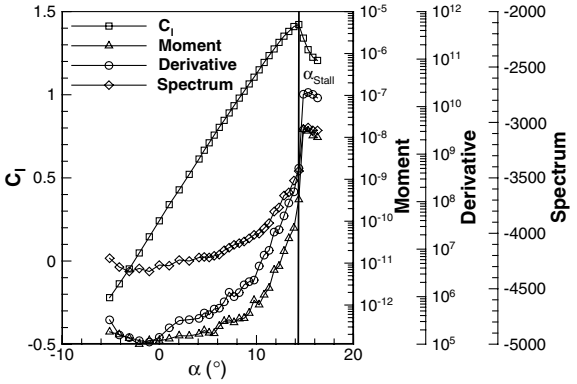

Fig. 1 Moment-, derivative-, and spectrum-based detector function outputs for the clean NACA 3415 model as a function of angle of attack.

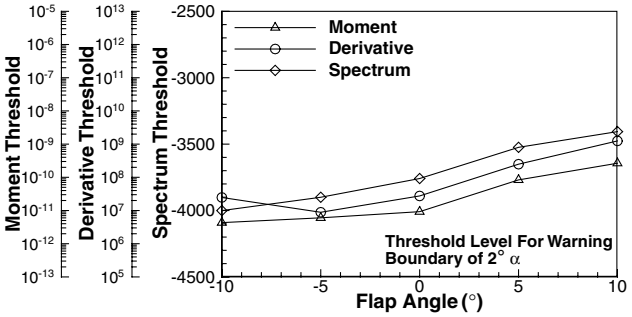

Fig. 3 Effect of flap angle on detector function threshold level with a warning boundary of 2° ($Re = 1.8 \times 10^6$).

structural incident with limited spanwise extent. Although the contamination affects the flow primarily downstream of the elements, the flap effectively integrates the flap hinge moments across the entire airfoil model span. The limited spanwise effect of the isolated contamination, combined with its midchord placement, resulted in a relatively small effect on the overall lift and stall angle. As a result, the region of premature separation downstream of the simulated upper-surface damage at moderate angles of attack produced an unsteady flowfield that led to increased detector function output levels while minimally reducing the lift and α_{stall} of the model (in comparison with the other contamination configurations). With this exception, a simple threshold can be set for each of the detector functions based on a warning boundary a set number of degrees before α_{stall}.

For the data shown, there appears to be sufficient signal in the detector function output to provide a boundary warning range of 1 to 4° before actual stall. For the data shown in Fig. 2, as an example, the threshold level was chosen to provide a warning 2° before stall. This single threshold (for each detector function) would appear to provide a relatively accurate warning boundary for all but the simulated upper-surface damage case. Overall, the detector functions developed work well across all the leading-edge cases tested.

The threshold level was observed to be a function of flap angle. The threshold level as a function of flap deflection for a stall warning boundary of 2° for each of the three detector functions is shown in Fig. 3 for the clean model. From Fig. 3, the threshold level is shown to be a moderate function of flap angle, with the threshold level generally increasing with increasing positive flap deflection.

For the proposed hinge-moment-based system, the individual stall boundary warnings produced by the three separate detector functions were averaged to provide a single stall boundary warning. The averaging of the three separate functions provided a level of redundancy to minimize the influence of outliers in the data that might appear in one of the detector functions. A standard deviation calculation between the three different methods computed in real time could also be used as a measure of the confidence in the stall boundary warning prediction.

Based on the threshold levels shown in Fig. 3 for an envelope boundary warning of 2° before stall, warnings were generated for the clean NACA 3415 model and the model with all six of the contaminants tested at $Re = 1.8 \times 10^6$ over the five flap deflections tested. The predicted stall warning boundaries for all configurations as a function of flap angle are shown in Fig. 4.

The results shown in Fig. 4 indicate the magnitude of the angle-of-attack warning before stall produced by the average of the three stall warning detector functions. A value of 2° would indicate a perfect prediction of stall angle of attack. A value above 2° indicates the detection algorithm produced a more conservative stall warning at an angle of attack lower than the set 2° before stall (providing more than 2° of warning), with a value below 2° indicating a less conservative boundary warning closer to stall than the set value, and therefore less warning. From Fig. 4, for the majority of the cases, the detection algorithm produces a warning within ±0.7° of the set value. The two cases that fall outside of this range are the upper-surface damage case and the rime-ice case for nonzero flap settings.

As mentioned previously, the upper-surface damage case did not exhibit detector function outputs that were consistent with the other configurations tested. Reasons for these differences were mentioned previously in this Note. The second outlying data set was the rime-ice case for nonzero flap deflections, where stall warning was provided approximately 2° before the 2° warning mark (4° before stall). This premature warning was due to the rime-ice case producing greater unsteadiness in the hinge moment output for nonzero flap deflections than the other cases. Additional investigation is required to identify why these two cases produced stall predictions that were inconsistent with the other configurations.

While boundary warning predictions were not generated for threshold boundaries other than 2°, there appears to be sufficient signal from the outputs of the detector functions to set the threshold boundary 1 to 4° before stall. However, from Fig. 2, the slope of the

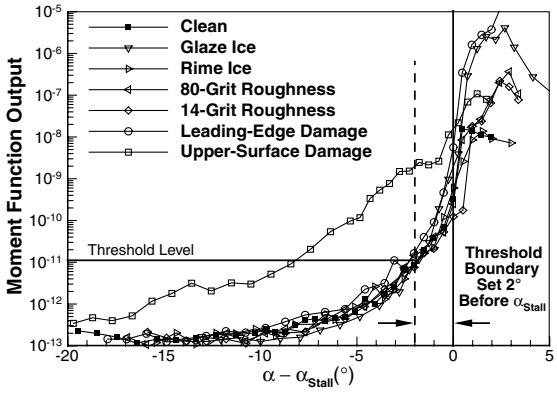

Fig. 2 Moment-based detector function output for the NACA 3415 under clean and contaminated configurations.

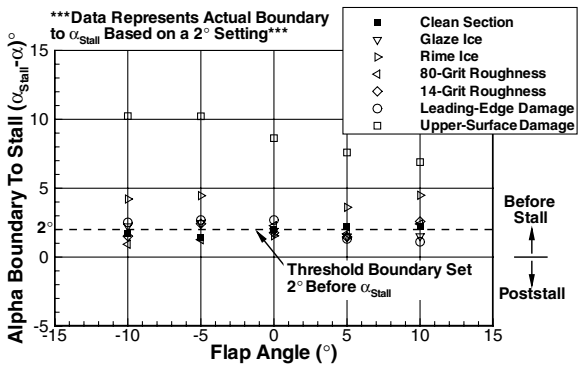

Fig. 4 Envelope boundary warning prediction under clean and contaminated configurations with a threshold boundary of 2°.

detector function outputs for the three detector functions (with respect to angle of attack to stall) were lower at 4° before stall than they were for 2° before stall. Because of this lower magnitude in slope, it is projected that a stall boundary of 4° may be accompanied by greater uncertainty in the stall prediction (greater than $\pm 0.7°$).

Conclusions

A stall prediction algorithm was developed that uses flap or control surface hinge moments to predict stall. The algorithm consisted of three detector functions, and it was developed using experimentally obtained hinge moment data from a NACA 3415 airfoil model. Data were taken for the clean airfoil model, as well as for six contaminated configurations. The detection algorithm used a threshold-based method for predicting stall, where detector function signals at the desired angle of attack before stall determined the threshold value. Based on the results obtained, there appears to be sufficient signal-to-noise ratio for five of the six cases to accurately set the stall warning boundary between 1 to 4° before stall. For the 2° warning boundary example, stall warnings within $\pm 0.7°$ of the set boundary were produced. The upper-surface contamination case provided overly conservative results, and additional research is underway to further understand this case and develop improved methods.

Acknowledgments

The authors wish to thank Mark Davis and the staff of NASA Dryden Flight Research Center for their contributions to this work. Support for this program was provided via Small Business Technology Transfer contract number NNX09CF549.

References

[1] Busch, G. T., Broeren, A. P., and Bragg, M. B., "Aerodynamic Simulation of a Horn-Ice Accretion on a Subscale Model," 45th AIAA Aerospace Sciences Meeting and Exhibit, Reno, NV, AIAA Paper 2007-0087, Jan. 2007.

[2] Luers, J., and Haines, P., "Heavy Rain Influence on Airplane Accidents," *Journal of Aircraft*, Vol. 20, No. 2, 1983, pp. 187–191. doi:10.2514/3.44850

[3] Shah, G. H., "Aerodynamic Effects and Modeling of Damage to Transport Aircraft," AIAA Atmospheric Flight Mechanics Conference and Exhibit, Honolulu, HI, AIAA Paper 2008-6203, Aug. 2008.

[4] Trunov, O. K., and Ingelman-Sundberg, M., "On the Problem of Horizontal Tail Stall Due to Ice," The Swedish-Soviet Working Group on Scientific-Technical Cooperation in the Field of Flight Safety Rept. JR-3, 1985.

[5] "Aircraft Accident Report: In-Flight Icing Encounter and Loss of Control Simmons Airlines, d.b.a American Eagle Flight 4184 Avions de Transport Regional (ATR) Model 72-212, N401AM, Roselawn, Indiana, October 31, 1994," U.S. National Transportation Safety Board Aviation Accident Rept. NTSB/AAR-96/01, Washington, D.C., July 1996.

[6] Gurbacki, H. M., and Bragg, M. B., "Sensing Aircraft Effects by Flap Hinge Moment Measurements," 17th Applied Aerodynamics Conference, Norfolk, VA, AIAA Paper 1999-3149, June 1999.

[7] Bragg, M. B., and Gurbacki, H. M., "Aircraft Surface Contamination Sensing System Using Control Surface Hinge Moment Measurements," U.S. Patent No. 6,140,942, 30 Oct. 2000.

[8] Ansell, P. J., "Flight Envelope Protection Using Flap Hinge Moment Measurement," M.S. Thesis, Univ. of Illinois at Urbana–Champaign, Urbana, IL, 2010.

[9] Ansell, P. J., Bragg, M. B., and Kerho, M. F., "Envelope Protection System Using Flap Hinge Moment Measurements," 28th Applied Aerodynamics Conference, Chicago, IL, AIAA Paper 2010-4225, June 2010.